Bull. Inst. Chem. Res., Kyoto Univ., Vol. 67, No. 2, 1989

Vibrational Modes of trans-1, 4-Polychloroprene by Neutron Incoherent Inelastic Scattering

Toshiji KANAYA*, Masatoshi OHKURA* and Keisuke KAJI*

Received June 3, 1989

Vibrational modes of trans-1, 4-polychloroprene have been investigated by neutron incoherent inelastic scattering. Amplitude-weighted frequency distribution which corresponds to density of phonon states was evaluated from the neutron spectrum. We also calculated the frequency distribution based on the results of the normal coordinate analysis by Petcavich and Coleman. By comparing the experimental and theoretical frequency distributions, we discuss assignments and dispersion relationships for the vibrational modes in the frequency range below 1000 cm^{-1}.

KEY WORDS: Neutron inelastic scattering/ trans-1,4-Polychloroprene/ Normal coordinate analysis/ Dispersion curve/ Amplitude-weighted frequency distribution/

INTRODUCTION

Extensive studies have been carried out on vibrational modes of trans-1, 4-polychloroprene (TPC) by infrared (IR) absorption[1-4] and Raman scattering[4] methods. Normal coordinate analysis has also been performed on an isolated chain of this polymer by Tabb and Koenig[5] and Petcavich and Coleman[4]. The results of Tabb and Keonig are in satisfactory agreement between the observed and calculated frequencies for these vibrations above 900 cm^{-1} but not below 900 cm^{-1}. The disagreements below 900 cm^{-1} have been attributed to the least reliability of the force constants associated with the chlorine atom. Petcavich and Coleman also carried out a similar calculation and obtained basic agreement with Tabb and Koeing above 900 cm^{-1} but several differences below 900 cm^{-1}. They pointed out that the out-of-plane C-Cl internal coordinates were undefined in the valence force field (VFF) of Tabb and Koenig. There remains ambiguity in the assignments of the vibrational modes below 900 cm^{-1}.

These two groups have reported the dispersion curves for the fundamental modes of TPC. Tabb and Koeing have concluded that there was very little coupling between adjacent translational repeat units of TPC because the branches were almost independent of phase angle. On the other hand, the results of Petcavich and Coleman show a considerable phase dependence even in the high frequency region above 900 cm^{-1}, indicating that some normal modes are coupled to adjacent units along the chain. It is impossible to observe dispersion relationship by IR and Raman spectroscopy. There hardly exist methods to measure the dispersion relationship except for neutron inelastic scattering. To our knowledge, however, no neutron

* 金谷利治, 大倉正寿, 梶 慶輔 : Laboratory of Fundamental Material Properties, Institute for Chemical Research, Kyoto University, Uji, Kyoto-fu 611, Japan.

inelastic scattering measurements on TPC have been reported.

In this work, we measure neutron incoherent inelastic scattering from TPC and compare with the results of the normal coordinate analysis in the frequency region below 1000 cm^{-1}.

EXPERIMENTAL

Sample. TPC was prepared from 2-chloro-1, 3-butadiene by a free radical emulsion polymerization and purified by precipitating from a benzen solution into an excess methanol. This polymer contains approximately 92% trans-1, 4, 6% cis-1, 4 and 2% 1, 2 and 3, 4 placements. For neutron scattering measurements, TPC was coated from a toluene solution on an outer surface of a hollow aluminum cylinder 140 mm high, 13.8 mm in diameter and 0.25 mm thick. The thickness of the coated film was controlled to be less than 0.15 mm, so that the multiple scattering from the film would be suppressed below 10%.

Measurements. Neutron scattering measurements were carried out with the time-of-flight (TOF) spectrometer LAM-D[6] installed at the National Laboratory for High Energy Physics, KEK, Tsukuba. The scattered neutrons with fixed energy (4.4 meV) were selected by PG (002) crystal analyzer and Be filter and detected by a He^3 counter. The measurements were made at 10K, 50K and 295K at the scattering angle 90°. After the measurements, we improved the spectrometer LAM-D to achieve higher energy resolution and higher counting rate. The measurement at 10K was reperformed with the improved LAM-D at the scattering angles 35° and 85°. The energy range covered by this spectrometer is below ca. 3000 cm^{-1} and the energy resolution ΔE is less than 10% of incident neutron energy E_0 for the old LAM-D and 6% for the improved LAM-D in the whole energy range.

Data analysis. After making corrections for background and incident neutron spectrum, observed TOF spectrum was converted to differential scattering cross-section $\partial^2\sigma/\partial\Omega\partial E$ which is defined as a probability that an incident neutron with energy E_0 is scattered into a solid angle $\partial\Omega$ and in an energy interval between E and $E+\partial E$. In the case of the present experiment, the observed differential scattering cross-section is mainly dominated by scattering of hydrogen atom, because TPC contains only three kinds of atoms, H, C and Cl, and incoherent atomic scattering cross-section of hydrogen atom is much larger than those of other atoms. Therefore, the observed differential scattering cross-section can be related to incoherent dynamic scattering law $S_{inc}(Q, \omega)$ through

$$\frac{\partial^2\sigma_{inc}}{\partial\Omega\partial E} = \frac{k_1}{k_0}(\langle b^2\rangle - \langle b\rangle^2)S_{inc}(Q, \omega) \qquad (1)$$

where k_0 and k_1 are the lengths of the wave vectors of incident and scattered neutrons $\boldsymbol{k}_0$ and $\boldsymbol{k}_1$, respectively. Q is the length of the scattering vector $\boldsymbol{Q}$ defined as $\boldsymbol{Q}=\boldsymbol{k}_0-\boldsymbol{k}_1$. b is the scattering length of hydrogen atom and $4\pi(\langle b^2\rangle-\langle b\rangle^2)$ corresponds to the incoherent atomic cross-section. Using eq. (1), we calculated incoherent dynamic scattering law $S_{inc}(Q, \omega)$.

For one phonon process, the incoherent differential scattering cross-section is given by

$$\frac{\partial^2\sigma_{inc}}{\partial\Omega\partial E} = \sum_{q,j}\frac{k_1}{k_0}\delta[\hbar\omega-\hbar\omega_j(\boldsymbol{q})]\frac{\hbar(n_s+1/2\pm1/2)}{2\omega_j(\boldsymbol{q})} \times\sum_{\rho}\frac{(\langle b_\rho^2\rangle-\langle b_\rho\rangle^2)}{M_\rho}|\boldsymbol{Q}\cdot\boldsymbol{U}_\rho^j(\boldsymbol{q})|^2 e^{-2W_\rho} \quad (2)$$

where $\hbar\omega_j(\boldsymbol{q})$ is phonon energy of the mode j with phonon wave vector $\boldsymbol{q}$. b_ρ is the scattering length of the atom at the position ρ, M_ρ its mass and e^{-2W} its Debye-Waller factor. $\boldsymbol{U}_\rho^j$ is a polarization vector representing the displacement of the atom for the phonon mode j. $n_s+1/2\pm1/2$ is Bose-Einstein population factor, where

$$n_s = \frac{1}{\exp[\hbar\omega_j(\boldsymbol{q})/k_BT]-1} \quad (3)$$

where k_B and T are the Boltzmann constant and absolute temperature, respectively. The upper sign refers to neutorn energy loss and the lower to energy gain. The upper sign was adopted for the present analysis because LAM-D is a down-scattering spectrometer. Using amplitude-weighted frequency distribution $G(\omega)$ (AWFD), eq. (2) is represented by

$$\frac{\partial^2\sigma_{inc}}{\partial\Omega\partial E} = \frac{k_0}{k_1}(\langle b^2\rangle-\langle b\rangle^2)\frac{Q^2}{2M}\hbar\left(n_s+\frac{1}{2}\pm\frac{1}{2}\right)e^{-2W}N\frac{G(\omega)}{\omega} \quad (4)$$

The amplitude-weighted frequency distribution with the Debye-Waller factor, $G(\omega)$ $exp(-2W)$ was calculated from eq. (4). The Debye-Waller factor does not seriously affect the low frequency range below 1000 cm^{-1}, especially for the low temperature measurements at 10K.

RESULTS AND DISCUSSION

TOF spectra measured with the old LAM-D at the scattering angle 90° are shown in Fig. 1 for 10K, 50K and 295K. These spectra are deformed by the energy distribution of incident neutrons, but give correct counting statistics. In the spectrum at 295K, any peak is not recognized except for two very broad peaks in the frequency ranges 10 to 100 cm^{-1} and 150 to 2000 cm^{-1}. It should be noted that the latter is spurious due to the energy distribution of incident neutrons and the former is attributable mainly to quasielastic scattering. On the other hand, in the spectrum of 10K, some sharp excitation peaks are observed and the intensity decreases extremely in the frequency range below 100 cm^{-1}. The difference of the spectra between 10K and 295K must be due to fluctuational motions by thermal agitations. It is easy to understand that the thermal fluctuational motions are effective in the low frequency range below 100 cm^{-1}, but difficult to understand in the high energy range because thermal energy k_BT is not large compared with excitation energies above 500 cm^{-1}. However, even in the high frequency range above 500 cm^{-1}, excitation peaks are also damped in the TOF spectrum of 295K. The extreme damping of the

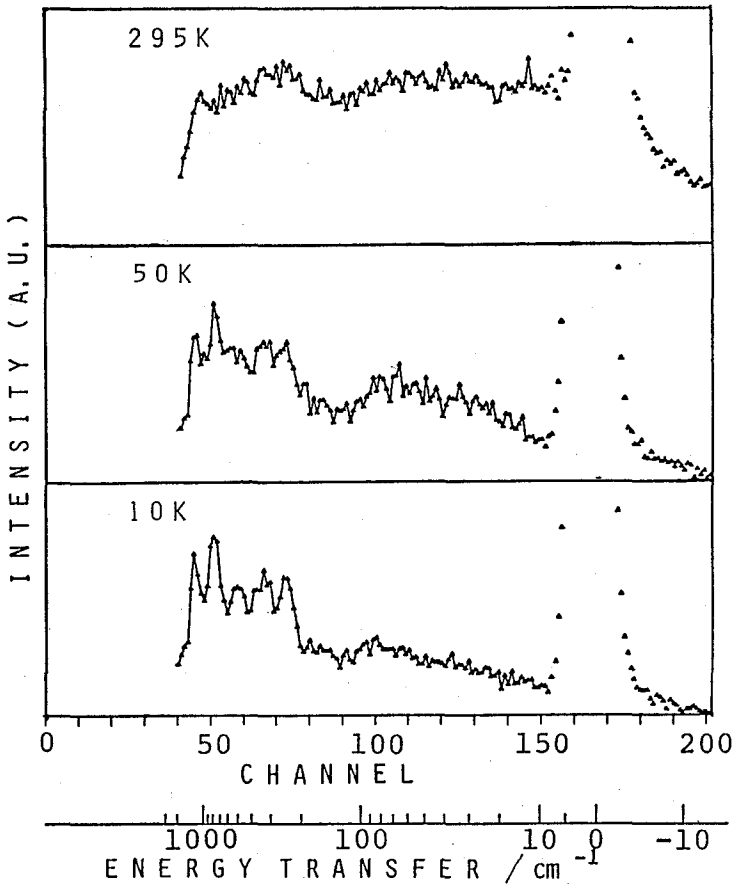

Fig. 1. TOF spectra of trans-1, 4-polychloroprene (TPC) measured with LAM-D at 10K, 50K and 295K. The scattering angle is 90°.

high energy excitation peaks must be caused from the measurement at high Q value, for example, $Q=8.0\text{Å}^{-1}$ at $\omega=1000\ \text{cm}^{-1}$ for the scattering angle 90°. For discussion of the fluctuational motions, dynamic scattering law is convenient because it gives Fourie transform of a probability that, when a scattering particle is at a position $\boldsymbol{r}=0$ at time $t=0$, it will exist at a position between $\boldsymbol{r}$ and $\boldsymbol{r}+d\boldsymbol{r}$ at time $t=t$. Dynamic scattering laws at 10K, 50K and 295K are shown in Fig. 2 which are normalized by the elastic peak intensity. $S(Q, \omega)$ at 295K is composed of sharp central elastic and wing broad quasielastic components. The quasielastic component can be represented by a Lorentz function in the frequency range below ca. $50\ \text{cm}^{-1}$. Relaxation time of the local fluctuational motion was evaluated from the width of the Lorentz function to be ca. 0.5 ps. On the other hand, quasielastic components in the dynamic scattering laws almost disappear at 10K and 50K, indicating that the thermal fluctuational motions are extremely suppressed.

The thermal fluctuational motions are one of the most significant problems to understand relaxation phenomena such as rheological and mechanical properties. However, it is beyond the purpose of this paper and will not be discussed hereafter.

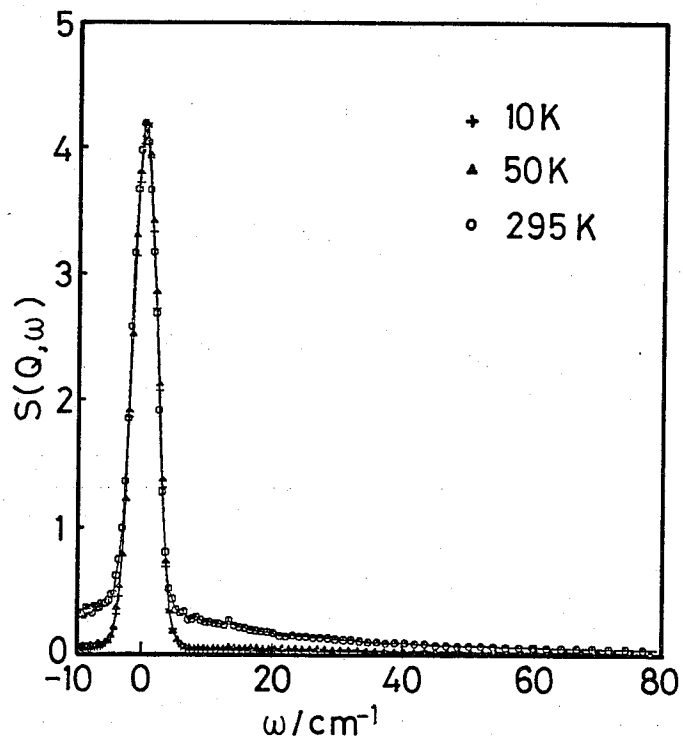

Fig. 2. Dynamic scattering laws $S(Q,\omega)$ of TPC at 10K (+), 50K (△) and 295K (○), normalized by the elastic peak intensity.

As the thermal fluctuations contaminate the inelastic scattering components, they are undesirable for the study of vibrational modes. Therefore, we employ the data measured at 10K to minimize the effects of the thermal fluctuations.

The amplitude-weighted frequency distributions (AWFD) were calculated from the neutorn TOF spectra measured with the improved LAM-D at the scattering angles 35° and 85°. The peaks in the AWFD at 35° are slightly sharper than those at 85° but the main feature is almost the same. Then, in order to get higher counting statistics, we summed up the two AWFDs. The result is shown in Fig. 3(a). This AWFD includes the Debye-Waller factor. However, we do not consider the effects because the Debye-Waller factor hardly deforms the spectrum of the low frequency range below 1000 cm^{-1}, especially for the measurement at 10K. The AWFD is proportional to the density of phonon states involving motions of hydrogen atoms. This gives "selection rules" in the neutron inelastic scattering process. The modes which do not involve any motion of the hydrogen atoms appear as weak peaks in the neutron spectrum.

The dispersion curves calculated by Petcavich and Coleman[4] are reproduced in the frequency range below 1000 cm^{-1} in Fig. 3(d). Some branches such as ν_5, ν_8, ν_9 and ν_{11}[7] exhibit distinct curvature in contrast to the results of Tabb and Koeing[5]. As will be discussed later, our results support the dispersion curves of Petcavich and Coleman. Using the dispersion curves, we calculated the frequency

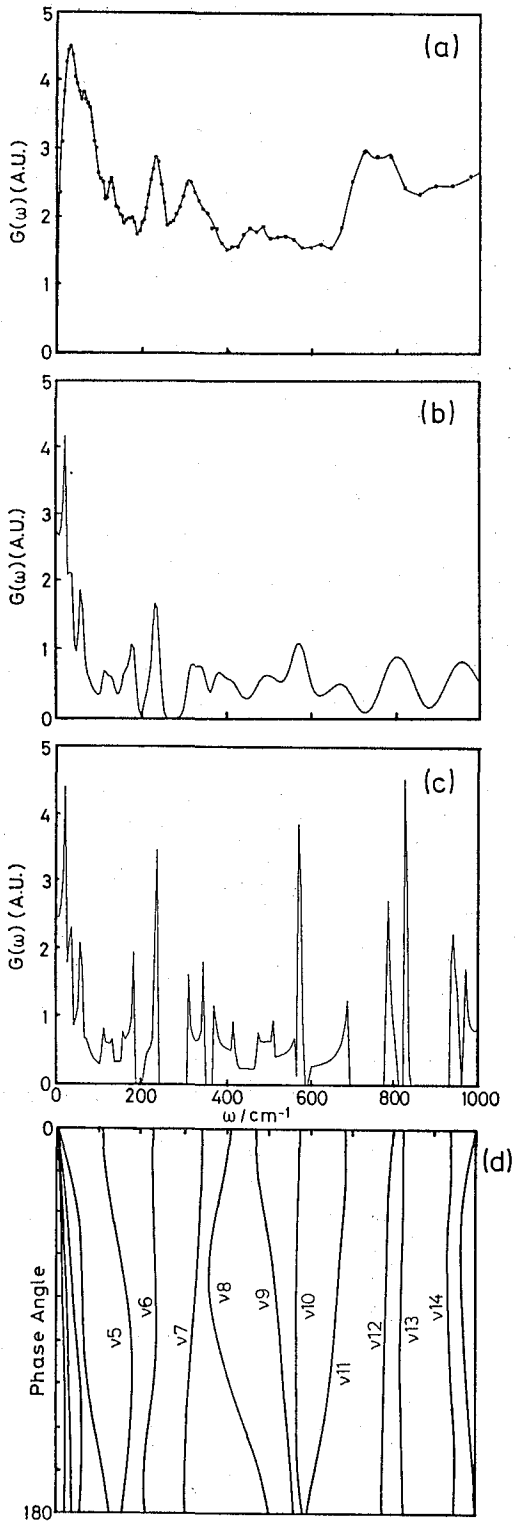

Fig. 3. (a) : Amplitude-weighted frequency distribution (AWFD) of TPC measured with LAM-D at 10K, which was obtained by summing up two AWFDs measured at the scattering angles 35° and 85°. (b): Frequency distribution of TPC obtained by convoluting the theoretical frequency distribution shown in (c) with the energy resolution function of LAM-D. (c): Frequency distribution of TPC calculated from the dispersion curves shown in (d). (d): dispersion curves of TPC for the fundamental modes below 1000 cm^{-1} after Petcavich and Coleman[4].

distribution by integrating the curves with the phase angle as shown in Fig. 3(c). In contrast to IR and Raman spectra, one branch does not always give a single peak in the frequency distribution. For example, the branch ν_7 which is predominantly assigned to C-C-Cl bending vibration gives two peaks at 313 cm^{-1} and 348 cm^{-1} in the frequency distribution. This property allows us to examine whether or not the dispersion curve has a distinct curvature. It should be noted that this theoretical frequency distribution is not the same as the AWFD measured by neutron inelastic scattering because the latter is weighted by atomic scattering cross-section and vibrational amplitude. This weighting is often a powerful tool for assignment of vibrational modes.

Peaks in the observed AWFD in Fig. 3(a) are very broad compared with the theoretical one in Fig. 3(c). It is due to the smearing effect of the energy resolution of the spectrometer.[6] The resolution function was convoluted with the theoretical frequency distribution and the result is shown in Fig. 3(b). This procedure will be described in detail elsewhere. The resultant spectrum is very broad and some peaks disappear by the smearing effect of the resolution. It is noted that the resolution becomes better as decreasing the frequency, so that the smearing effects are more pronounced in higher frequency range.

A summary of the observed frequencies and the assignments of the normal modes of TPC by Petcavich and Coleman[4] are listed in Table 1 below 1000 cm^{-1}. The theoretical assingments were made from the potential energy distribution in each

Table 1. Neutron band frequency below 1000 cm^{-1} of trans-1, 4-polychlororprene in comparison with infrared spectroscopy and normal coordinate analysis.

Neutron (cm^{-1})		IR (cm^{-1})		Approximate potential energy distribution[b),c)]
Observed	Calculated[a)]	Observed[b)]	Calculated[b)]	
—	958	958	942	21%K_T, 17%H_ω, 35%H_θ, −16%$F_{R\omega}$
790	803	826	826	10%H_θ, 27%τ_D, 36%Γ_2
740		780	794	79%H_γ, 17%H_θ, −15%$f_{\gamma\gamma}$
—	668	671	684	12%K_K, 34%H_ω, 13%H_ε, 10%H_β, 14%τ_D
—	570	577	572	71%K_K
484	498	477	471	16%K_T, 11%H_ω, 57%Γ_1
453				
—	385	407	409	46%H_ω, 24%τ_D, 17%Γ_2
314	330	339	349	31%H_ε, 41%H_α
233	235	253	225	34%H_ε, 35%H_β
175	180	153	103	11%K_T, 12%H_ω, 42%τ_R
128	118			
65	60	—	—	
32	23	—	—	

a) obtained from the frequency distribution convoluted with the resolution function of LAM-D (see Fig. 3(b)).
b) reproduced from Petcavich and Coleman.[4]
c) internal coordinate and force constant notations follow Petcavich and Coleman.[4]

normal vibration, which were calculated with respect to each force constant. In the low frequency range below 1000 cm^{-1} there are some differences between the theoretical assignments of Petcavich and Coleman[4] and Tabb and Koenig[5], especially for the modes observed in IR spectra at 826, 671, 577 and 477 cm^{-1}. Tabb and Koenig has assigned the band at 826 cm^{-1} to the stretching of C-Cl, while Petcavich and Coleman predominantly to the CH out-of-plane bending. The latter assignment agrees with the results of the group frequency approach by Mochel and Hall.[1] In the neutron AWFD, we observe an intense broad peak at 790 cm^{-1} which should include the mode observed at 826 cm^{-1} in IR spectrum. This intense peak supports the assignment of Petcavich and Coleman because the stretching of C-Cl does not give such strong intensity. The frequency 790 cm^{-1} is slightly lower than the IR measurement. This fact suggests that the dispersion curve of this mode has a distinct curvature, probably the lower the frequency the higher the phase angle. The assignment of the 780 cm^{-1} band in the IR spectrum to the CH_2 rocking is not open to doubt and the intense peak around 740 cm^{-1} in the neutron AWFD should include the mode.

The 671 cm^{-1} band in the IR spectrum has been assigned to the CH out-of-plane bending by Tabb and Koenig, but to a highly mixed mode with contributions from the C-Cl stretching, C-C-C bending and C=C twisting by Petcavich and Coleman. On the other hand, the neutron AWFD has no peak near this frequency, indicating this band does not include the large motion of hydrogen atom. The 577 cm^{-1} band has been assigned to the C-Cl stretching vibration by Petcavich and Coleman. This assignment is consistent with the observation of Mochel and Hall[1]. In the neutron AWFD, no peaks are observed near 577 cm^{-1}. This fact suggests that the mode is also concerned with motion of chlorine atom.

The two weak peaks observed at 484 and 453 cm^{-1} in the neutron AWFD should correspond to the peak at 477 cm^{-1} in the IR spectrum, which was assigned to the C-Cl out-of-plane bending by Petcavich and Coleman. This observation indicates that the mode includes the motions of hydrogen atoms more or less and the dispersion curve has such curvature to give two peaks in the frequency distribution.

Some distinct peaks are observed in the low frequency range below 450 cm^{-1} of the neutron AWFD, though Petcavich and Coleman have not discussed about them. The peak observed at 314 cm^{-1} should be assigned to the C-C-Cl bending vibrational mode according to the calculation of Petcavich and Coleman. High energy tail of this peak should include the C-C-C bending mode observed at 407 cm^{-1} in the IR spectrum, though the mode cannot be recognized as a peak in the neutron AWFD. As shown in Fig. 3(c), these two modes are distinguishable in the theoretical frequency distribution while the the peak of the C-C-C bending mode is broadened due to the marked curvature of the dispersion curve (see Fig. 3(d)). Furthermore, the effect of the energy resolution smears the peak, such as being almost impossible to recognize as a peak, as shown in Fig. 3(b). This prediction agrees with our observation and we confirm that the dispersion curve of the C-C-C bending mode has a distinct curvature.

The peak at 233 cm^{-1} in the neutron AWFD is assigned to the C=C—C bending

according to the calculation of Petcavich and Coleman. The peaks at 175 and 128 cm^{-1} are probably due to the single mode assinged to the C-C torsional vibration, including the small contribution from the acoustic mode. In the frequency range below 100 cm^{-1}, peaks at 65 and 23 cm^{-1} are observed in the neutron AWFD. It is no meaning to compare these modes with the theoretical calculation because it was done on a single chain, neglecting the lattice modes which are dominant in the low frequency range.

ACKNOWLEGEMENT

We are indebted to Professor K. Inoue, Hokkaido University, for support and advice throughout this study.

REFERENCES AND NOTE

(1) W.E. Mochel and M.B. Hall, *J. Am. Chem. Soc.*, **71,** 4082 (1949).
(2) M.M. Coleman, P.C. Petcavich, D.L. Tabb and J.L. Koenig, *J, Polym. Sci. Polym. Letters Ed.*, **12,** 577 (1974).
(3) D.L. Tabb, J.L. Koenig and M.M. Coleman, *J. Polym. Sci. Polym. Phys. Ed.*, **13,** 1145 (1975).
(4) R.J. Petcavich and M.M. Coleman, *J. Macromol. Sci. -Phys.*, **B18,** 47 (1980).
(5) D.L. Tabb and J.L. Koenig, *J. Polym. Sci. Polym. Phys. Ed.*, **13,** 1159 (1975).
(6) K. Inoue, K. Kaji, Y. Kiyanagi, T. Kanaya, H. Iwasa and N. Nishida, *Bull. of the Faculty of Engineering, Hokkaido University,* **128,** 85 (1985).
(7) Branches are numbered sequencially starting from zero cm^{-1}, according to Petcavich and Coleman[4].